Z. Phys. D – Atoms, Molecules and Clusters 14, 307–315 (1989)

Atoms, Molecules
Zeitschrift für Physik D and Clusters

Coherent laser excitation of Rydberg states in a weak static magnetic field

G. Alber
Fakultät für Physik, Albert-Ludwigs-Universität, Hermann-Herder-Strasse 3, D-7800 Freiburg i.Br., Federal Republic of Germany

Received 11 Juli 1989; final version 22 September 1989

We study one-photon excitation of atomic Rydberg- and continuum states close to a photoionization threshold in the presence of a weak static external magnetic field. A semiclassical closed orbit representation for the atomic transition amplitudes is derived, which exhibits the connection between quantum mechanics and the classical dynamics of the excited electron whose motion under the combined influence of the Coulomb field of the ionic core and the magnetic field is chaotic.

PACS 32.80.Rm; 32.60.+i

1. Introduction

Recently a theory of laser excitation of atomic Rydberg- and continuum states close to a photoionization threshold has been developed, which is based on the observation, that for optical frequencies and sufficiently small laser intensities, $I \ll 1.4 \times 10^{17}$ W/cm^2, the atom-laser interaction is localized in a finite *reaction zone* [1, 2]. Typically, this region extends a few Bohr radii around the atomic nucleus and is therefore small in comparison with the extent of highly excited Rydberg states. If, in addition, the excitation process is also localized in time, because the characteristic excitation time (i.e. the pulse duration or the depletion time of the initial state) is short in comparison with the classical orbit times of the excited Rydberg states, many Rydberg- and continuum states are coherently exicted and a radial electronic wave packet is generated [3, 4]. So far, applications of this theory have concentrated on cases, where outside the reaction zone the atomic Hamiltonian is separable [2, 4, 5].

The application of semiclassical methods and the corresponding relations between quantum- and classical mechanics in Hamiltonian systems, which are not separable or integrable, has been an active field of research for many years [6–11]. In particular, Gutzwiller's periodic orbit formula [7], in which, within a semiclassical framework, the density of states of a nonseparable system is expressed as a sum of contributions of all periodic orbits, clearly exhibits these connections. In a pioneering work recently Du and Delos [12] and Bogomolny [13] have applied similar semiclassical methods to the description of photoabsorption processes in hydrogen. Motivated by recent experiments [14, 15], they investigated laser excitation of hydrogen by a long and weak pulse in the presence of a static magnetic field in the energy region close to the photoionization threshold [16]. Analogous to Gutzwiller's periodic orbit formula, they represented the (energy averaged) photoabsorption cross section in the classically chaotic regime as a sum of contributions of all isolated, unstable closed orbits which start from the nucleus.

In this paper we extend our previous work and study one-photon excitation of an atom close to the photoionization threshold in the presence of a weak external static magentic field. In particular, we are interested in excitation by a short or intense laser pulse, so that the excitation process cannot be described by a time independent photoabsorption cross section and an electronic wave packet is generated. Using ideas of Quantum Defect Theory (QDT), in the case of a weak external magnetic field we can distinguish between three characteristic spatial regions as far as the dynamics of the excited electron is concerned [17], namely the *reaction zone*, the surrounding *Coulomb zone*, where the dynamics of the excited electron is dominantly determined by the

Coulomb force of the ionic core and the *asymptotic zone*, where the external field is at least as important as the Coulomb field of the ionic core. By using quantum-defect-type matching procedures and solving the problem in the nonseparable asymptotic zone semiclassically, we derive analytical expressions for various transition amplitudes. They can be represented as a sum of contributions of all isolated, unstable closed orbits of the excited electron which start from the reaction zone. Within this framework we discuss nonhydrogenic core effects as well as effects originating from depletion of the initially occupied atomic state.

In Sect. II we derive the basic equations describing one-photon excitation of Rydberg- and continuum states close to threshold from an energetically low-lying bound state. Thereby the quantity of central importance is the self-energy of the initial state, for which we derive a closed orbit representation, which is asymptotically valid in the limit of weak external magnetic fields. With the help of this result in Sect. III we discuss coherent laser excitation of Rydberg- and continuum states by a short or intense laser pulse.

2. Basic equations

In this section we derive a semiclassical closed-orbit representation for the atomic self-energy, which describes one-photon excitation of atomic Rydberg- and continuum states close to a photoionization threshold.

We consider one-photon excitation of atomic Rydberg states from an energetically low lying bound state $|g>$ of energy ε_g, which is assumed to be nondegenerate. The atom is placed in a weak, external magnetic field of field strength B, whose influence on the bound state $|g>$ is negligible. However, at large distances from the nucleus the magnetic field eventually starts to dominate the Coulomb field of the ionic core and thus significantly influences Rydberg and continuum states close to the photoionization threshold [17].

Assuming an instantaneous turn-on of the laser pulse at $t=0$ and neglecting photon absorption from the excited states, in the dipole- and rotating wave approximation the initial state probability amplitude at time t is given by (in Hartree atomic units) [2]

$$a_g(t)=1/2\pi \int_{-\infty+i0}^{\infty+i0} \mathrm{d}\varepsilon \mathrm{e}^{-\mathrm{i}(\varepsilon-\omega)t} a_g(\varepsilon) \tag{1}$$

with $a_g(\varepsilon)=i[\varepsilon-\varepsilon_g-\omega+\delta\omega_p-\Sigma(\varepsilon)]^{-1}$. The resonant part of the self-energy of the initial state $|g>$ is given by

$$\Sigma(\varepsilon)=<g|\boldsymbol{\mu}\cdot\mathbf{e}^*\mathscr{E}^*[\varepsilon-H_A+i0]^{-1}\boldsymbol{\mu}\cdot\mathbf{e}\mathscr{E}|g> \tag{2}$$

and $\delta\omega_p=|\mathscr{E}|^2\omega^{-2}$ is the Stark-shift (ponderomotive shift [18]) of the excited states. The parameters $\mathbf{e}$, ω and $\mathscr{E}$ are the polarization, frequency and field strength of the exciting laser pulse, respectively. The atomic dipole operator is $\boldsymbol{\mu}$ and H_A is the atomic Hamiltonian, which describes the dynamics of the excited electron in the external field. For simplicity, we restrict our discussion to an atom with only one valence electron. The Hamiltonian of the excited electron is given by

$$H_A(\mathbf{x},\gamma)=-1/2\,\Delta_x+V(\mathbf{x},\gamma)+V_{\mathrm{par}}(\mathbf{x}) \tag{3}$$

with $V(\mathbf{x},\gamma)=V_c(\mathbf{x})+V_{\mathrm{dia}}(\mathbf{x})$. Due to the finite extent of the ionic core, the effective electrostatic potential $V_c(\mathbf{x})$ deviates from a pure $-1/r$ Coulomb potential within a typical distance of a few Bohr radii around the atomic nucleus [19]. The influence of the external magnetic field on the dynamics is characterized by the dimensionless parameter $\gamma=\dfrac{\hbar\omega_L}{2Ry}=B/4.70\times10^{-5}T^{-1}$ with the Larmor frequency ω_L. The para- and diamagnetic interaction terms are $V_{\mathrm{par}}(\mathbf{x})=-\gamma L_z$ and $V_{\mathrm{dia}}(\mathbf{x})=1/2\gamma^2 r^2\sin^2\theta$, respectively. The z-component of the angular momentum is L_z with the z-axis parallel to the homogeneous magnetic field.

The main problem in calculating various laser excitation amplitudes is the evaluation of the self-energy $\Sigma(\varepsilon)$, which is related to the solution, $F_\varepsilon(\mathbf{x})$, of the inhomogeneous Schrödinger equation [1, 20]

$$[\varepsilon+i0-H_A(\mathbf{x},\gamma)]\,F_\varepsilon(\mathbf{x})=\mathbf{x}\cdot\mathbf{e}<\mathbf{x}|g> \tag{4}$$

by

$$\Sigma(\varepsilon)=|\mathscr{E}|^2\int \mathrm{d}^3x <g|\mathbf{x}>\mathbf{x}\cdot\mathbf{e}^* F_\varepsilon(\mathbf{x}). \tag{5}$$

As $|g>$ is an energetically low lying bound state, the self-energy is determined by the behaviour of $F_\varepsilon(\mathbf{x})$ within a distance of a few Bohr radii around the atomic nucleus.

The solution of (4) is facilitated by noting that there are three characteristic spatial regimes as far as the dynamics of the excited electron is concerned. The atom-laser interaction is localized in a region of the size of the initial bound state $|g>$ and therefore typically extends a distance r_c of the order of a few Bohr radii around the atomic nucleus [1]. This *reaction zone* is surrounded by a *Coulomb zone* ($r_c<r\ll a=\gamma^{-2/3}$), in which the Coulomb field of the ionic core and the paramagnetic interaction term $V_{\mathrm{par}}(\mathbf{x})$ are dominant. In the surrounding *asymptotic zone* ($r\gtrsim a$) the diamagnetic interaction term $V_{\mathrm{dia}}(\mathbf{x})$ is no longer negligible and significantly modifies the dynamics of the excited electron [17]. This physical distinction allows to solve the Schrödinger equation by a step-

wise procedure. In a first step (4) may be solved in each region separately and in a second step these local solutions are matched together.

In the asymptotic part of the Coulomb zone ($1 \ll r \ll a$) the general solution of (4), which is regular for $r \to 0$, is given by [2]

$$F_\varepsilon(\mathbf{x}) \sim \sum_{l,m} Y_l^m(\theta,\varphi)\frac{1}{r}[1/2\,\Phi_{\varepsilon_m l}^{(+)}(r)\,\mathscr{B}_{lm} + \mathscr{F}_{\varepsilon_m l}(r)\,\mathscr{A}_{lm}(\varepsilon)] = \sum_m [\psi_{\text{out}}^{(m)}(r,\theta) + \psi_{\text{in}}^{(m)}(r,\theta)]\,\mathrm{e}^{\mathrm{i}m\varphi} \tag{6}$$

with $\varepsilon_m = \varepsilon + \gamma m$. The transition amplitudes $\mathscr{B}_{lm} = 2i\pi\mathscr{D}_{lm}^{(-)}$ determine a particular solution of the inhomogeneous equation (4) with the complex photoionization dipole matrix elements $\mathscr{D}_{lm}^{(-)} = -\int \mathrm{d}^3x\, 1/r \mathscr{F}_{\varepsilon_m l}(r)\, Y_l^{m*}(\theta,\varphi)\,\mathbf{x}\cdot\mathbf{e} < \mathbf{x}|g>$. As these dipole matrix elements get their dominant contribution from a region of a few Bohr radii around the atomic nucleus they are approximately energy- and field-independent close to threshold. $\mathscr{F}_{\varepsilon_m l}(r)$ is an energy normalized solution of the homogeneous part of (4). Semiclassically, its asymptotic form is given by

$$\mathscr{F}_{\varepsilon_m l}(r) \sim 1/2[\Phi_{\varepsilon_m l}^{(-)}(r) - \Phi_{\varepsilon_m l}^{(+)}\chi_l] \quad (1 \ll r) \tag{7}$$

with

$$\Phi_{\varepsilon_m l}^{(\pm)}(r) = \sqrt{\frac{2}{\pi p_r}}\,\mathrm{e}^{\pm \mathrm{i}[w_{\varepsilon_m}(r_<, r) - (l+1/2)\pi + \pi/4]}, \tag{8}$$

where $w_{\varepsilon_m}(r_<, r)$ is the radial classical action of zero angular momentum. p_r and l are the radial- and angular momenta of the electron. The scattering matrix elements χ_l describe elastic scattering of the valence electron inside the core region due to the presence of the residual core electrons. This scattering process can only affect low angular momentum states of the excited electron with $l < l_0$, which have a sufficiently large overlap with the ionic core. Therefore we may write

$$\chi_l = 1 + f_l \tag{9}$$

with $f_l = 0$ for $l > l_0$. The wavefunction $\psi_{\text{out(in)}}^{(m)}(r,\theta)$ represents the outgoing or incoming part of $\mathscr{F}_\varepsilon(\mathbf{x})$, which is proportional to $\Phi_{\varepsilon_m l}^{(+)}(r)$ or $\Phi_{\varepsilon_m l}^{(-)}(r)$ respectively. In the absence of an external field the Coulomb zone extends to infinity and according to standard procedures of QDT the complex amplitudes $\mathscr{A}_{lm}(\varepsilon)$ are determined by the requirement that $F_\varepsilon(\mathbf{x})$ has to remain finite for $r \to \infty$ [2, 19]. According to (5) the self-energy is related to these amplitudes by

$$\Sigma(\varepsilon) = \Sigma^{(s)} + |\mathscr{E}|^2 \sum_{lm} \mathscr{D}_{lm}^{(+)}\,\mathscr{A}_{lm}(\varepsilon) \tag{10}$$

with the recombination dipole matrix elements $\mathscr{D}_{lm}^{(+)} = \int \mathrm{d}^3x < g|\mathbf{x} > \mathbf{x}\cdot\mathbf{e}^*\, Y_l^m(\theta,\varphi)\, 1/r \mathscr{F}_{\varepsilon_m l}(r)$ and $\Sigma^{(s)} = \delta\omega - i\Gamma/2$. The shift $\delta\omega$ is a quadratic Stark shift contribution and $\Gamma = 2\pi \sum_{lm} |\mathscr{D}_{lm}^{(-)}\mathscr{E}|^2$ is the total ionization rate of $|g>$ according to Fermi's Golden rule. The quantity $\Sigma^{(s)}$ characterizes the atom-laser interaction inside the finite reaction zone and is therefore approximately independent of energy and magnetic field strength as long as $|\varepsilon|, \gamma \ll 1$ [2].

For the evaluation of the self-energy of (10) we have to determine the unknown amplitudes $\mathscr{A}_{lm}(\varepsilon)$. For this purpose we solve the Schrödinger equation (4) in the asymptotic zone and match this solution with $F_\varepsilon(\mathbf{x})$ in the asymptotic part of the Coulomb zone. Taking advantage of the cylindrical symmetry of the problem and introducing scaled coordinates $\tilde{\mathbf{x}} = \mathbf{x}/a$ and energies $\tilde{\varepsilon} = \varepsilon/\gamma^{2/3}$, we therefore have to solve the boundary value problem

$$\left[-\frac{1}{\lambda^2}\,1/2\,\Delta_{\tilde{\mathbf{x}}} + V(\tilde{\mathbf{x}}, \gamma = 1) - \tilde{\varepsilon}_m\right]\psi^{(m)}(\tilde{r},\theta) = 0 \tag{11}$$

in the region $\tilde{r} > r_0$ with the boundary condition

$$\psi^{(m)}(\tilde{r},\theta)|_{\tilde{r}=r_0} = \psi_{\text{in}}^{(m)}(ar_0,\theta) + \psi_{\text{out}}^{(m)}(ar_0,\theta), \quad (1/a \ll r_0 \ll 1) \tag{12}$$

where $\lambda = \sqrt{a} = \gamma^{-1/3}$ is a measure for the order of magnitude of the classical actions involved in the problem. In the case of a weak magnetic field, i.e. $\gamma \ll 1$, and for energies close to threshold, i.e. $|\tilde{\varepsilon}| \lesssim 1$, we may solve (11) asymptotically in the limit $\lambda \gg 1$ with semiclassical methods as developed by Maslov and Fedoriuk [21].

In order to construct this asymptotic solution we start from the outgoing part of the boundary condition $\psi_{\text{out}}^{(m)}(r,\theta)$, which involves a rapidly oscillating radial function and a slowly varying function of θ. The function $\psi_{\text{out}}^{(m)}(r,\theta)$ therefore determines the one-dimensional Lagrangian manifold $L_1^{(m)} = \{(\tilde{r}, \theta_0, \tilde{p}_r, \tilde{p}_\theta)|\tilde{r} = r_0, \quad 0 < \theta_0 < \pi, \quad \tilde{p}_r = \sqrt{2(\tilde{\varepsilon}_m + 1/\tilde{r})}, \tilde{p}_\theta = 0\}$ [21]. Propagating $L_1^{(m)}$ through phase space along the Hamiltonian flow generated by the Hamiltonian

$$H^{(m)} = 1/2[\tilde{p}_r^2 + \tilde{p}_\theta^2/\tilde{r}^2 + m^2\lambda^{-2}/(\tilde{r}^2\sin^2\theta)] - 1/\tilde{r} + 1/2\tilde{r}^2\sin^2\theta \tag{13}$$

we obtain the two-dimensional Lagrangian manifold $L_2^{(m)} = \{(\tilde{r}(\tau,\theta_0),\ \theta(\tau,\theta_0),\ \tilde{p}_r(\tau,\theta_0),\ \tilde{p}_\theta(\tau,\theta_0))|0 < \theta_0 < \pi, 0 < \tau < T\}$. Here, T is some large time of interest, which is determined e.g. by the pulse duration of the

laser. The asymptotic solution of (11) at point $\tilde{\mathbf{x}}$ is then given by [21]

$$\psi^{(m)}(\tilde{r},\theta)=\sum_j \sqrt{J(0,\theta_{0j})/|J(\tau_j,\theta_{0j})|}\cdot e^{i(\lambda S_{\varepsilon_m}(\tau_j,\theta_{0j})-m\pi\nu_j-\mu_j\pi/2)}\psi^{(m)}_{\text{out}}(ar_0,\theta_{0j}). \tag{14}$$

The summation index j represents a sum over all projections of $L_2^{(m)}$ onto the two-dimensional configuration space at point $(\tilde{r},\theta)$ and

$$S^{(m)}_{\varepsilon_m}(\tau_j,\theta_{0j})=\int_0^{\tau_j} d\tau\left[\tilde{p}_r\frac{d\tilde{r}}{d\tau}+\tilde{p}_\theta\frac{d\theta}{d\tau}\right] \tag{15}$$

is the classical action along trajectory j, which starts at point (r_0,θ_{0j}) with $\tau=0$ and reaches point $(\tilde{r},\theta)$ with $\tau=\tau_j$. In (14) we have used the fact that the term involving the z-component of the angular momentum m in the Hamiltonian of (13) is negligible unless the electron is reflected at the z-axis and θ becomes small. Therefore, in the limit $\lambda\gg 1$ we have approximately $S^{(m)}_{\varepsilon_m}(\tau_j,\theta_{0j})=S_{\varepsilon_m}(\tau_j,\theta_{0j})+m\pi\nu_j\lambda^{-1}$, with ν_j beeing the number of reflections at the z-axis and $S_{\varepsilon_m}(\tau_j,\theta_{0j})\equiv S^{(m=0)}_{\varepsilon_m}(\tau_j,\theta_{0j})$. The amplitudes of the asymptotic wave function are determined by the projection of the Lagrangian manifold $L_2^{(m)}$ onto configuration space at point $(\tilde{r},\theta)$, i.e.

$$J(\tau_j,\theta_{0j})=\left.\frac{d\tilde{x}\wedge d\tilde{y}\wedge d\tilde{z}}{d\tau\wedge d\theta_0\wedge d\varphi}\right|_{(\tau_j,\theta_{0j})}=\tilde{r}^2\sin\theta\left.\frac{d\tilde{r}\wedge d\theta}{d\tau\wedge d\theta_0}\right|_{(\tau_j,\theta_{0j})}. \tag{16}$$

μ_j is the Morse index of trajectory j for $\tilde{r}>r_0$ [21].

The unknown amplitudes $\mathscr{A}_{lm}(\varepsilon)$ of (10) are determined by the requirement that $\psi^{(m)}(\tilde{r},\theta)$ has to fulfil the boundary condition of (12), which implies

$$\mathscr{A}_{lm}(\varepsilon)=2\pi\int_0^\pi d\theta\sin\theta\, Y_l^m(\theta,0)^*(-1)^l e^{i2w_{\varepsilon_m}(r<,ar_0)}\cdot\sum_j\sqrt{J(0,\theta_{0j})/|J(\tau_j,\theta_{0j})|}\cdot e^{i|\lambda S_{\varepsilon_m}(\tau_j,\theta_{0j})-m\pi\nu_j-(\mu_j+1)\pi/2|}\cdot\sum_{l'}Y_{l'}^m(\theta_{0j},0)(-1)^{l'}[\mathscr{B}_{l'm}-\chi_{l'}\mathscr{A}_{l'm}(\varepsilon)] \tag{17}$$

with $\tilde{r}(\tau_j,\theta_{0j})=r_0,\tau_j>0$. Equation (17) may be solved iteratively with the starting value $\mathscr{A}^{(0)}_{lm}(\varepsilon)=0$. In the limit $\lambda\gg 1$, $e^{i\lambda S_{\varepsilon_m}(\tau_j,\theta_{0j})}|_{\tilde{r}=r_0}$ is a rapidly oscillating function of θ in comparison with the rest of the integrand and $\mathscr{A}^{(1)}_{lm}(\varepsilon)$ may be evaluated with the method of stationary phase. The dominant contributions thereby arise from final angles θ_j with $\frac{\partial S_{\varepsilon_m}}{\partial\theta}|_{(r_0,\theta_j)}=\tilde{p}_\theta(r_0,\theta_j)=0$. Noting that $\frac{\partial\tilde{p}_\theta}{\partial\theta}|_{(r_0,\theta_j)}>0$ for $\tilde{p}_r(r_0,\theta_j)<0$ we find

$$\mathscr{A}^{(1)}_{lm}(\varepsilon)=i(2\pi)^{3/2}\sum_j\sqrt{\sin\theta_j\sin\theta_{0j}}\,Y_l^m(\theta_j,0)^*(-1)^l\cdot(\lambda|M^{(j)}_{21}|)^{-1/2}e^{i[\lambda S_j(\varepsilon_m)-m\pi\nu_j-(\mu_j+2)\pi/2+\pi/4]}\cdot\sum_{l'}Y_{l'}^m(\theta_{0j},0)(-1)^{l'}\mathscr{B}_{l'm}. \tag{18}$$

The sum now includes all closed trajectories j of the Hamiltonian $H^{(0)}$ of (13) starting at $\tilde{r}=0$. $S_j(\varepsilon_m)$ are their classical actions. The symplectic monodromy matrix $M^{(j)}$ is evaluated at $\tilde{r}=r_0$ and characterizes the separation of trajectories in the neighbourhood of the closed orbit j, i.e.

$$\begin{pmatrix}\Delta\theta\\ \Delta\tilde{p}_\theta\end{pmatrix}=\begin{pmatrix}M_{11}&M_{12}\\ M_{21}&M_{22}\end{pmatrix}\begin{pmatrix}\Delta\theta_0\\ \Delta\tilde{p}_{\theta_0}\end{pmatrix}. \tag{19}$$

Taking into account (9), the second iterate $\mathscr{A}^{(2)}_{lm}(\varepsilon)$ consists of two parts: The first term corresponds to the replacement $\chi\to 1$ on the r.h.s. of (17) and is of the order of $O(\lambda^{-1/2})$. The second term involves the scattering amplitudes f_l and describes effects due to elastic scattering of the excited electron inside the core region. Typically $f_l\neq 0$ only for low values of the angular momentum l, so that this contribution to $\mathscr{A}^{(2)}_{lm}(\varepsilon)$ is of the order of $O(\lambda^{-1})$ and may therefore be neglected in the limit $\lambda\gg 1$. Thus, neglecting electron-ion scattering inside the core region also in all higher iterations, we finally find

$$\mathscr{A}_{lm}(\varepsilon)=-\sum_j\sum_{n_j}(2\pi)^{5/2}\sqrt{\sin\theta_j\sin\theta_{0j}}\,Y_l^m(\theta_j,0)^*(-1)^l\cdot\left(\lambda\left|M^{(j)}_{21}\frac{\sinh(n_j u_j)}{\sinh u_j}\right|\right)^{-1/2}\cdot e^{i[n_j(\lambda S_j(\varepsilon_m)-m\pi\nu_j-(\mu_j+2)\pi/2)+\pi/4]}\cdot\sum_{l'}Y_{l'}^m(\theta_{0j},0)(-1)^{l'}\mathscr{D}^{(-)}_{l'm} \tag{20}$$

with n_j indicating the number of returns of the j-*th* trajectory to the reaction zone. In the derivation of eqn. (20) we have used the relation

$$\sum_l Y_l^m(\theta_1,0)\,Y_l^m(\theta_2,0)^*\approx 1/(2\pi)\,\delta(\theta_1-\theta_2)/\sin\theta_1,$$

which is exact for $m=0$ and approximately also valid for small values of m. Furthermore, we have taken into account that the required matrix element of the

Table 1. Emission- (return-)angle $\theta_0(\theta)$, action S, orbit time T, monodromy matrix element M_{21}, stability exponent u, Morse index $\mu+2$, number of crossings of z-axis ν and multiplicities of closed orbits with $T<4.5\ \pi/\gamma$ at $\varepsilon=0$ as evaluated by Wintgen [23]

Orbit	θ_0	θ	S	$T\times\gamma$	M_{21}	u	$\mu+2$	ν	mult
I_1	90.0	90.0	5.782	2.094	2.816	1.317	3	0	1
I_2	53.832	53.832	8.580	4.935	10.969	2.892	5	1	2
I_3	42.810	42.810	10.213	8.111	24.360	3.743	7	2	2
I_4	37.311	37.311	11.428	11.288	39.272	4.239	9	3	2
IIb_0	63.649	116.351	12.537	6.739	31.637	3.897	7	2	2
IIa_1	81.677	128.246	14.233	7.427	56.826	4.291	8	1	2
IIa_1	51.754	98.323	14.233	7.427	56.826	4.291	8	1	2
IIb_1	46.679	112.505	14.513	9.568	67.944	4.756	9	3	2
IIb_1	67.495	133.321	14.513	9.568	67.944	4.756	9	3	2
IIa_2	79.114	138.459	15.777	10.878	107.925	4.937	10	2	2
IIa_2	41.541	100.886	15.777	10.878	107.925	4.937	10	2	2
IIb_2	39.602	110.506	15.884	12.521	97.671	5.144	11	4	2
IIb_2	69.494	140.398	15.884	12.521	97.671	5.144	11	4	2
III_1	60.270	60.270	16.158	9.066	108.283	5.144	9	3	2

n_j-*th* iterate of the symplectic matrix $M^{(j)}$ is given by [13]

$$|(M^{nj})^{(j)}_{21}| = |M^{(j)}_{21}| \frac{\sinh(n_j u_j)}{\sinh u_j}. \tag{21}$$

The stability exponent $u_j \geqq 0$ of the unstable closed orbits are related to the eigenvalues $\lambda_j^{(1,2)}$ of $M^{(j)}$ by $|\lambda_j^{(1,2)}| = e^{\pm u_j}$. Inserting (20) into (10), we obtain for the self-energy

$$\Sigma(\varepsilon) = \Sigma^{(s)} - |\mathscr{E}|^2 (2\pi)^{5/2} \sum_m \sum_{jn_j} \sqrt{\sin\theta_j \sin\theta_{0j}} \cdot \left(\lambda \left| M^{(j)}_{21} \frac{\sinh(n_j u_j)}{\sinh u_j} \right|\right)^{-1/2} \cdot e^{i[n_j(\lambda S_j(\varepsilon_m) - m\pi\nu_j - (\mu_j+2)\pi/2) + \pi/4]} d_m^+(\theta_j)\, d_m^-(\theta_{0j}) \tag{22}$$

with the recombination- and photoionization dipole matrix elements $d_m^+(\theta_j) = \sum_l Y_l^m(\theta_j, 0)^*(-1)^l \mathscr{D}_{lm}^{(+)}$ and $d_m^-(\theta_{0j}) = \sum_l Y_l^m(\theta_{0j}, 0)(-1)^l \mathscr{D}_{lm}^{(-)}$.

Equation (22) is the main result of this section. It expresses the atomic self-energy as a sum of contributions of all unstable closed orbits of the classical Hamiltonian $H^{(0)}$ of (13), which start from $\tilde{r}=0$. These trajectories have already been studied numerically in great detail [12, 22]. According to (22), the following classical properties of orbit j are important: The emission- and return angles θ_{0j} and θ_j, the classical action S_j, the monodromy matrix element $M^{(j)}_{21}$ together with the stability exponent u_j and the Morse index μ_j+2 together with the number of crossings of the z-axis ν_j. Table 1 summarizes these parameters for closed orbits with $T<4.5\ \pi/\gamma$ at $\varepsilon=0$ [23]. The derivation of (22) shows, that in the limit $\lambda \gg 1$ nonhydrogenic core effects are only important in the initial excitation and final recombination process, which are characterized by the dipole matrix elements $d_m^-(\theta_{0j})$ and $d_m^+(\theta_j)$. The imaginary part of (22) is proportional to the photoabsorption cross section. In particular, in the hydrogenic limit it reduces to the result which has previously been derived by Bogomolny [13].

3. Results and discussion

Using the asymptotic expression for the atomic self-energy as given in (22), we study coherent one-photon excitation of atomic Rydberg- and continuum-states close to threshold by a short or intense laser pulse in the presence of a static magnetic field.

3.1. Short pulse

We assume that the exciting laser pulse of field strength $\mathscr{E}_1(t)$, frequency ω_1 and polarization $\mathbf{e}_1$ is so short, that the initial state $|g>$ is not significantly depleted and many Rydberg- and continuum states are coherently excited. This implies that the influence of the laser field on the atom may be taken into account perturbatively and an electronic wave packet is generated, which is well localized with respect to its radial coordinate in comparison with the typical extent of highly excited Rydberg states [3, 4]. The time evolution of this electronic wave packet can be probed e.g. by a second time delayed short laser pulse of field strength $\mathscr{E}_2(t)$, frequency ω_2 and polarization $\mathbf{e}_2$, which induces a transition to some other energetically low lying bound state $|f>$ with energy ε_f [4]. The probability of finding the atom in state $|f>$ is large, whenever a part of the initially generated wave

packet returns again to the reaction zone, where the stimulated recombination process takes place. This way we are able to probe the motion of the electronic wave packet as it propagates under the combined influence of the Coulomb force of the positively charged ionic core and the external static magnetic field.

Assuming Gaussian envelopes for both laser pulses with pulse duration τ, i.e.

$$\mathscr{E}_i(t)=\mathscr{E}_i \exp\left[-1/(2\tau^2)(t-t_i)^2\right],$$

$i=1, 2$, we find for the final state probability long after the interaction with both laser pulses in second order perturbation theory

$$|<f|\psi>_t|^2=\left|1/(2\pi i)\int_{-\infty}^{\infty} d\varepsilon e^{-i\varepsilon(t_2-t_1)}\Sigma_{fg}(\varepsilon)\cdot\tilde{\mathscr{E}}_1(\varepsilon-\varepsilon_g-\omega_1)\tilde{\mathscr{E}}_2^*(\varepsilon-\varepsilon_f-\omega_2)\right|^2 \quad (23)$$

with the Fourier-transforms of the laser pulses $\tilde{\mathscr{E}}_i(\Delta)=\int_{-\infty}^{\infty} dt\mathscr{E}_i(t)e^{i\Delta(t-t_i)}$. In (23) we have assumed that the mean time delay between both laser pulses, t_2-t_1, is large in comparison with their durations. The generalized self energy

$$\Sigma_{fg}(\varepsilon)=<f|\mathbf{x}\cdot\mathbf{e}_2^*[\varepsilon-H_A+i0]^{-1}\mathbf{x}\cdot\mathbf{e}_1|g> \quad (24)$$

may be evaluated asymptotically in the limit $\lambda\gg 1$ with the methods described in section II. In particular, if both pulses are not too short so that dispersion of the excited wave packet is negligible, i.e. $n_j\gamma^{-5/3}\frac{\partial^2 S_j}{\partial\tilde{\varepsilon}^2}|_{\bar{\varepsilon}}(1/\tau^2)\ll 1$, we may linearize the classical action around the mean excited energy $\bar{\varepsilon}=\varepsilon_g+\omega_1$. Using (22) and assuming that the second laser is tuned on resonance, i.e. $\bar{\varepsilon}=\varepsilon_f+\omega_2$, we obtain for the final state probability

$$|<f|\psi>_t|^2=\Big|\sum_m\sum_{j,n_j}(2\pi)^{3/2}d_m^+(\theta_j)\sqrt{\sin\theta_j\sin\theta_{0j}}\cdot\left(\lambda\left|M_{21}^{(j)}\frac{\sinh(n_j u_j)}{\sinh u_j}\right|\right)^{-1/2}\cdot e^{i[n_j(\lambda S_j(\varepsilon_m)-m\pi\nu_j-(\mu_j+2)\pi/2)+\pi/4]}d_m^-(\theta_{0j})\cdot\tau\mathscr{E}_1\mathscr{E}_2^*2\pi^{3/2}e^{-(t_2-t_1-n_jT_{\varepsilon_m}^{(j)})^2/(4\tau^2)}\Big|_{\varepsilon=\bar{\varepsilon}}^2 \quad (25)$$

with the classical orbit time $T_{\varepsilon_m}^{(j)}=\gamma^{-1}\frac{\partial S_j}{\partial\tilde{\varepsilon}}|_{\varepsilon_m}$ of orbit j.

Figures 1 show the final state probability as a function of the time delay between both laser pulses in the case of laser excitation of p-states of sodium at the (zero-field) photoionization threshold. For simplicity we assume that $\mathscr{E}_1=\mathscr{E}_2$ and that both laser pulses are linearly polarized in the same direction. θ_{pol} is the angle between the laser polarization and the magnetic field axis. The initial and final state are assumed to be the same s-state. The magnetic field strength is $B=0.47$ T. As the pulse duration τ is less than the classical orbit time of the fastest closed orbit I_1 (see Table 1), the laser excitation process is not only localized in space but also in time and an electronic wave packet is generated, which is well localized with respect to the extension of the classically accessible region. As soon as this wave packet enters the asymptotic zone it is broken up and performs a complicated motion under the combined influence of the Coulomb field of the positively charged ionic core and the magnetic field. The maxima in Fig. 1 correspond to returns of various fractions of the initially prepared wave packet to the reaction zone, where the laser-atom interaction is localized and where the second probe pulse may induce a transition to the final state $|f>$, whenever the (mean) time delay between both pulses, t_2-t_1, is a multiple of the classical orbit time of one of the closed orbits. The form of the recombination peaks reflects the laser pulse profiles and their heights are determined by the monodromy-matrix elements $|M_{21}^{(j)}|$ of these orbits. In the evaluation of Fig. 1 we have included the closed orbits, whose parameters are summarized in Table 1 for $\varepsilon=0$. Their form and the corresponding recombination peaks are schematically shown in Fig. 1 (see also [22, 23]). The photoionization- and recombination dipole matrix elements of sodium are related to the total ionization rate of the initial s-state, Γ, by

$$2\pi\mathscr{D}_{lm}^{(+)}\mathscr{D}_{lm}^{(-)}|\mathscr{E}|^2/\Gamma=e^{i2\pi\alpha}\begin{cases}1/2\sin^2(\theta_{pol}) & (|m|=1)\\ \cos^2(\theta_{pol}) & (m=0)\end{cases}$$

with the nonhydrogenic core effects characterized by the approximately energy- and field independent quantum defect $\alpha=0.854$ of the excited p-states [19]. However, according to (25) this quantum defect gives only rise to a global phase factor, which does not affect the final state probability.

In Fig. 1a the polarization of both laser pulses is perpendicular to the direction of the applied magnetic field. All recombination peaks can be attributed to repeated returns of the generated wave packet to the reaction zone. The first two recombination peaks correspond e.g. to the first and second return of the Edmonds-Garton-Tomkins orbit I_1 [14, 22] and the third peak is due to the first return of orbit I_2. In Fig. 1b the angle between the laser polarization and the magnetic field axis is 45°. The angular distribution of the initially prepared wave packet is now different,

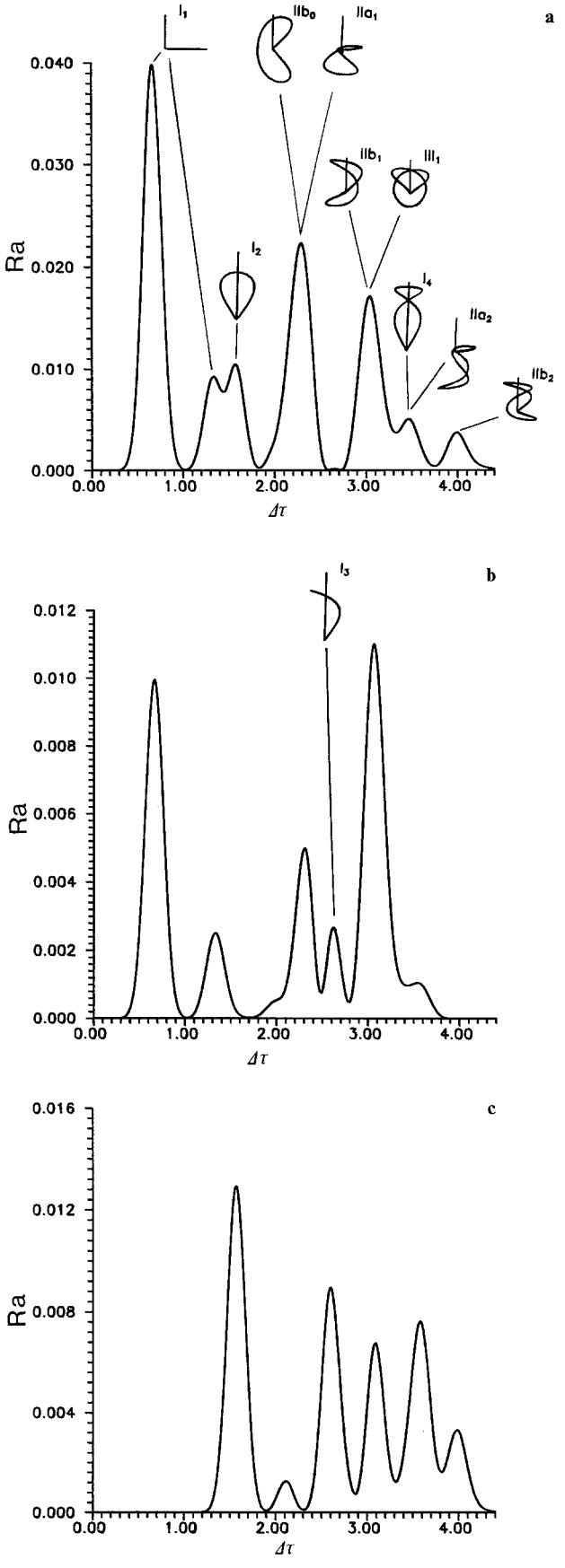

which leads to a change of the relative importance of the various recombination peaks. The most significant difference to Fig. 1a is the disappearance of the recombination peaks associated with the first returns of orbits I_2 and IIb_2. This is due to almost complete destructive interference between the $m=0$- and $m=\pm 1$-contributions of the corresponding transition amplitudes. In Fig. 1c the laser polarization is parallel to the magnetic field and the angular distribution of the generated wave packet is concentrated around the magnetic field axis. As there is no electron emission perpendicular to the magnetic field axis, the contribution of the orbit I_1 is missing.

3.2. *Intense laser pulse*

If the exciting laser pulse is so intense that the initial state $|g>$ is depleted, the excitation process can no longer be described perturbatively. However, under the conditions discussed in Sect. II the time evolution of the initial state probability amplitude can be obtained from (1), (2) and (22). Expanding $a_g(\varepsilon)$ to lowest order in the asymptotic parameter $\lambda \gg 1$, we obtain

$$a_g(\varepsilon) = i(\varepsilon-\bar{\varepsilon}+i\Gamma/2)^{-1} - i(\varepsilon-\bar{\varepsilon}+i\Gamma/2)^{-1}|\mathscr{E}|^2 \cdot (2\pi)^{5/2} \sum_m \sum_{j n_j} \sqrt{\sin\theta_j \sin\theta_{0j}} \cdot \left(\lambda \left| M_{21}^{(j)} \frac{\sinh(n_j u_j)}{\sinh u_j} \right|\right)^{-1/2} \cdot e^{i[n_j(\lambda S_j(\varepsilon_m) - m\pi\nu_j - (\mu_j+2)\pi/2)+\pi/4]} \cdot d_m^+(\theta_j)\, d_m^-(\theta_{0j})(\varepsilon-\bar{\varepsilon}+i\Gamma/2)^{-1} + O(\lambda^{-1}) \quad (26)$$

with the mean excited energy $\bar{\varepsilon} = \varepsilon_g + \omega + \delta\omega - \delta\omega_p$. The neglected terms of order $O(\lambda^{-1})$ describe effects of laser assisted electron-ion scattering inside the reaction zone. In the limit $\lambda \gg 1$ these terms are expected to be small and are neglected in the following. Furthermore, if the exciting laser pulse is not too intense, i.e. $\gamma^{-5/3} \frac{\partial^2 S}{\partial \bar{\varepsilon}^2}|_{\bar{\varepsilon}} \Gamma^2 \ll 1$, the energy integrals in (1), may

Fig. 1a–c. Raman-transtition probability $\mathrm{Ra} = |<f|\psi>_t|^2/(\Gamma\tau)^2$ as a function of $\Delta\tau = (t_2 - t_1)/(\pi/\gamma)$ for $\gamma = 10^{-6}$, $\tau = 0.1\ \pi/\gamma$ and different polarization angles θ_{pol}. The form of the closed orbits is schematically shown on top of the corresponding recombination peaks. The straight lines indicate the direction of the magnetic field. **a**: $\theta_{\mathrm{pol}} = 90°$; **b**: $\theta_{\mathrm{pol}} = 45°$; **c**: $\theta_{\mathrm{pol}} = 0°$

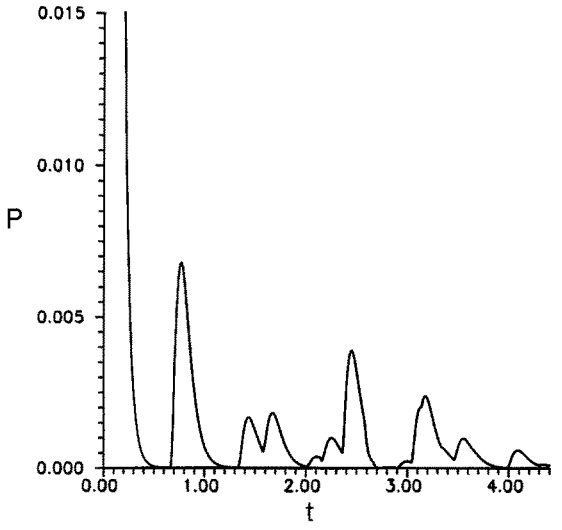

Fig. 2. Initial state probability $P=|a_g(t)|^2$ as a function of interaction time t in units of (π/γ) for $\gamma=10^{-6}$, $\theta_{\text{pol}}=90°$ and $\Gamma=20\,\gamma/\pi$

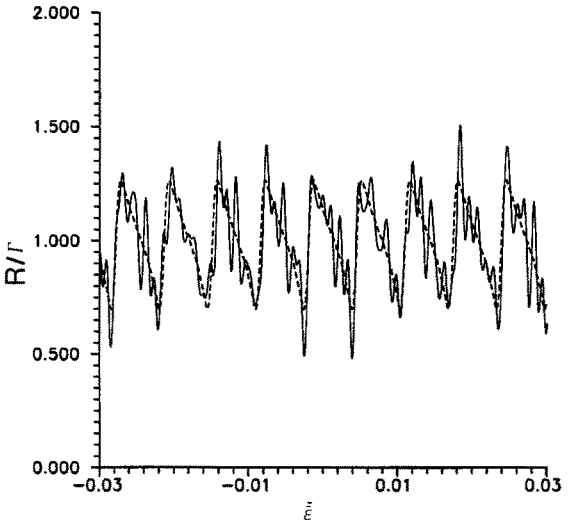

Fig. 3. Excitation rate R/Γ as a function of the scaled energy $\tilde{\varepsilon}=(\varepsilon_g+\omega+\delta\omega-\delta\omega_p+\gamma)\,\gamma^{-2/3}$ for p-states of sodium ($\alpha=0.854$)

be evaluated by linearizing the classical action $S_j(\varepsilon_m)$ around the mean excited energy $\bar{\varepsilon}$. So we finally find

$$
\begin{aligned}
a_g(t)=&\,\mathrm{e}^{-\mathrm{i}(\bar{\varepsilon}-\omega)t-\Gamma t/2}+i(2\pi)^{5/2}\\
&\cdot\sum_m\sum_{jn_j}[|\mathscr{E}|^2\,d_m^+(\theta_j)\,d_m^-(\theta_{0j})]/(\Gamma/2)\sqrt{\sin\theta_j\sin\theta_{0j}}\\
&\cdot\left(\lambda\left|M_{21}^{(j)}\frac{\sinh(n_j u_j)}{\sinh u_j}\right|\right)^{-1/2}\\
&\cdot\mathrm{e}^{\mathrm{i}[n_j(\lambda S_j(\varepsilon_m)-m\pi\nu_j-(\mu_j+2)\pi/2)+\pi/4]}\\
&\cdot\mathrm{e}^{-\mathrm{i}(\bar{\varepsilon}-\omega)t}\,\mathrm{e}^{-\Gamma/2(t-n_j T_{\varepsilon_m}^{(j)})}\,(\Gamma/2)(t-n_j\,T_{\varepsilon_m}^{(j)})\\
&\cdot\Theta(t-n_j\,T_{\varepsilon_m}^{(j)})|_{\varepsilon=\bar{\varepsilon}}.
\end{aligned}
\tag{27}
$$

The various terms in the sum over n_j in (27) may be attributed to repeated returns of the excited electron back to the reaction zone along orbit j. With each return the laser pulse may induce a transition to the initial state thus increasing $a_g(t)$. In particular, if the exciting laser pulse is intense, so that the depletion time of the initial state, $1/\Gamma$, is short in comparison with the shortest classical orbit time $T_{\varepsilon_m}^{(j)}$, the various contributions of (27) are separated in time. Physically this reflects the fact that the intense laser pulse generates an electronic wave packet, parts of which return again to the reaction zone well separated in time.

Figure 2 shows the initial state probability as a function of the interaction time. An intense laser pulse excites p-states of sodium around $\bar{\varepsilon}=0$ with quantum defect $\alpha=0.854$ from an energetically low lying s-state. The depletion time of the initial state, $1/\Gamma$, is shorter than the classical orbit time of the Edmonds-Garton-Tomkins orbit I_1 so that a Rydberg wave packet is generated. For times $t\ll T_{\bar{\varepsilon}}^{(j)}$ the wave packet has not yet moved away very far from the reaction zone, where it has been generated, and therefore behaves like in an ionization process. This manifests itself in an exponential decay of the initial state probability with rate Γ [2]. Eventually parts of this wave packet return again to the reaction zone thereby increasing the initial state probability by stimulated recombination. Apart from the exponential decay, Fig. 2 looks very similar to Fig. 1. The only major difference is the form of the recombination peaks, which reflects the pulse form of the exciting laser pulse.

If the pulse duration is long in comparison with some of the classical orbit times, many terms in the sum over j_j in (27) contribute. In particular, if the initial state is not significantly depleted, i.e. $\Gamma\tau\ll 1$, the excitation process may be characterized by the time independent rate

$$
\begin{aligned}
R=&\frac{\mathrm{d}}{\mathrm{d}t}(1-|a_g(t)|^2)|_{t=\tau}=-2\,\mathrm{Im}[\Sigma(\bar{\varepsilon})]\\
=&\,\Gamma\{1+2(2\pi)^{5/2}\sum_m\sum_{jn_j}\sqrt{\sin\theta_j\sin\theta_{0j}}\\
&\cdot\left(\lambda\left|M_{21}^{(j)}\frac{\sinh(n_j u_j)}{\sinh u_j}\right|\right)^{-1/2}\\
&\cdot\mathrm{Im}[\mathrm{e}^{\mathrm{i}[n_j(\lambda S_j(\varepsilon_m)-m\pi\nu_j-(\mu_j+2)\pi/2)+\pi/4]}\\
&\cdot d_m^+(\theta_j)\,d_m^-(\theta_{0j})]\,|\mathscr{E}|^2/\Gamma\}_{\varepsilon=\bar{\varepsilon}}.
\end{aligned}
\tag{28}
$$

The first term of (28) gives the "direct" contribution to the excitation rate and the remaining terms represent contributions of successive returns of the excited electron to the reaction zone. The quantum mechanical interference between the corresponding excitation amplitudes manifests itself in the energy dependence of R, which is particularly sensitive to

phase shifts arising from quantum defects of the excited Rydberg- and continuum states.

Figure 3 shows the excitation rate R as a function of the mean excited energy. P-states of sodium with $m=1$ are excited from an energetically low lying s-state by right circularly polarized light. The magnetic field strength is $B=4.7$ mT ($\gamma=10^{-8}$). The pulse duration is $\tau=4.4\,\pi/\gamma$, so that only terms with $n_j\,T_{\varepsilon m}^{(j)}<\tau$ contribute to the sum of (28). The dashed curve shows the contribution of the Edmonds-Garton-Tomkins orbit including contributions of multiple returns, which give rise to an asymmetric lineshape. In particular, from (28) we notice that the elastic electronion scattering inside the core region, which is characterized by the quantum defect of the excited p-channel, leads to a shift of the lineshapes in comparison with the corresponding hydrogenic results.

Conclusion

We have studied laser excitation of an atom close to a photoionization threshold in the presence of a weak static magnetic field. Within a semiclassical framework we have discussed the time dependent aspects of the laser excitation process and effects originating from a nonhydrogenic core. With the help of a semiclassical closed-orbit formula we have expressed the transition amplitudes as a sum of contributions arising from all unstable closed orbits of the excited electron, which start from the reaction zone. This representation exhibits the connections between quantum mechanics and the complicated classical dynamics of the excited electron. It has been shown that the generation of an electronic wave packet by a short or intense laser pulse offers the possibility of probing the time evolution of the excited electron under the combined influence of the Coulomb field of the ionic core and the static magnetic field.

Stimulating discussions with E.B. Bogomolny, D. Wintgen and P. Zoller are gratefully acknowledged.

References

1. Giusti, A., Zoller, P.: Phys. Rev. A **36**, 5178 (1987)
2. Alber, G., Zoller, P.: Phys. Rev. A **37**, 377 (1988)
3. Parker, J., Stroud C.R. Jr.: Phys. Rev. Lett. **56**, 716 (1986)
4. Alber, G., Ritsch, H., Zoller, P.: Phys. Rev. A **34**, 1058 (1986)
5. Alber, G.: Phys. Rev. A **40**, 1321 (1989)
6. Balian, R., Bloch, C.: Ann. Phys. **85**, 514 (1974)
7. Gutzwiller, M.C.: J. Math. Phys. **12**, 343 (1971)
8. Berry, M.V., Mount, K.E.: Rep. Prog. Phys. **35**, 315 (1972)
9. Heller, E.J.: Phys. Rev. Lett. **53**, 1515 (1984)
10. Delos, J.B.: Adv. Chem. Phys. **65**, 161 (1986)
11. Bogomolny, E.B.: Physica D **31**, 169 (1988)
12. Du, M.L., Delos, J.B.: Phys. Rev. A. **38**, 1896; 1913 (1988)
13. Bogomolny, E.B.: Pis'ma Zh. Eksp. Teor. Fiz. **47** 445 (1988) [JETP Lett. **47**, 526 (1988)]
14. Garton, W.R.S., Tomkins, F.S.: Astrophys. J. **158**, 839 (1968)
15. Holle, A., Wiebusch, G., Main, J., Hager, J., Rottke, H., Welge, K.H.: Phys. Rev. Lett. **56**, 2594 (1986)
16. For a comprehensive list of references of experimental and theoretical work on the problem of Hydrogen in a static magnetic field see Friedrich, H., Wintgen, D.: Phys. Rep. (in press)
17. O'Mahony, P.F.: Fundamental processes of atomic dynamics. Briggs, J.S., Kleinpoppen, H., Lutz, H.O. (eds), p. 197. New York: Plenum 1987
18. Mittleman, M.H.: Phys. Rev. A **29**, 2245 (1984)
19. Seaton, M.J.: Rep. Prog. Phys. **46**, 167 (1983)
20. Dalgarno, A., Lewis, J.T.: Proc. R. Soc. A **233**, 70 (1955)
21. Maslov, V.P., Fedoriuk, M.V.: Semiclassical approximation in quantum mechanics. Boston: Reidel 1981
22. Wintgen, D., Friedrich, H.: Phys. Rev. A **36**, 131 (1987)
23. Wintgen, D.: Private communication